

# Seismic Response of Viaducts Accounting for Soil-Structure Interaction



**S. Carbonari, M. Morici**

*Università Politecnica delle Marche, Italy*

**F. Dezi**

*University of San Marino, San Marino*

**G. Leoni**

*University of Camerino, Italy*

**C. Nuti**

*University of Rome 3, Italy*

**F. Silvestri, G. Tropeano**

*University of Naples Federico II, Italy*

**I. Vanzi**

*The G. d'Annunzio University, Italy*

## SUMMARY:

A research was recently granted by the Italian Government to develop a comprehensive procedure to account for spatial variability of ground motion as well as soil-structure interaction in assessing the behaviour of bridges. This paper reports on the work-package relevant to the effects of soil-structure interaction. In the first section, a methodology to include the effects of soil-structure interaction in the nonlinear response of bridges is presented. Kinematic interaction analysis is performed in the frequency domain by means of a procedure accounting for radiation damping, soil-pile and pile-to-pile interaction; the non-linear inertial interaction analysis is performed in the time domain by using a finite element model of the superstructure. Suitable lumped parameter models are implemented to reproduce the frequency-dependent compliance of soil-foundation systems. In the second section, some results of nonlinear dynamic analyses performed on some bridges designed on soft soils by means of a direct displacement approach are presented.

*Keywords: Bridges, Lumped parameter models, Nonlinear behaviour, Pile foundation, Soil-structure interaction*

## 1. INTRODUCTION

Site geomorphology and the interaction with the soil may significantly affect the seismic response of structures as demonstrated by field evidences. Fixed base structural models, commonly used for design purposes, cannot capture the real dynamic structural behaviour being unable to describe the deformability and dissipative capability of the soil-foundation system. Furthermore, in cases such as highway and railway viaducts, the foundations may be placed on non homogeneous soils so that the seismic shaking may vary between the different supports (Nuti and Vanzi, 2005). In such cases, soil-structure interaction and non-synchronous seismic inputs have to be considered in the analyses (Sextos et al., 2003). In principle, modern codes such as Eurocode 8, require specific analyses including such effects to be performed with different degrees of accuracy depending on the importance of the structure. Even if models and analysis procedures are available, an integrated methodology does not exist yet. A research was recently granted by the Italian Government to develop a comprehensive procedure to account for spatial variability of ground motion as well as Soil-Structure Interaction (SSI) in assessing the behaviour of bridges. In this framework, the paper focuses on the effects of soil-structure interaction.

In the first section, a procedure to include the effects of SSI in the nonlinear response of bridges is presented. This is based on the domain decomposition technique: kinematic interaction analysis is performed in the frequency domain by means of a procedure accounting for radiation damping, soil-pile and pile-to-pile interaction; the nonlinear inertial interaction analysis is performed in the time domain by using a finite element model of the superstructure. Suitable Lumped Parameter Models

(LPMs) are implemented to reproduce the frequency-dependent compliance of the soil-foundation systems. In the second section, some results of nonlinear dynamic analyses performed on a set of bridges designed on soft soils by means of a direct displacement approach are presented. Three pier heights are chosen by imposing different ductility demands. The seismic responses are compared with those given by fixed base models demonstrating at what extent, soil-structure interaction is important.

## 2. METHODOLOGY FOR SSI ANALYSIS

SSI analysis is performed by means of the substructure method by dividing the soil-foundation-structure system (Fig. 1a) into the superstructure and the soil-foundation sub-systems (Fig. 1b). The kinematic interaction analysis of the soil-foundation sub-system is performed to evaluate the Foundation Input Motion (FIM) and the stress resultants in piles due to the propagation of seismic waves in the soil. The seismic response of the superstructure (inertial interaction analysis) is evaluated by considering compliant restraints at the pier bases and the FIM calculated in the previous step. Although the method is based on the superposition principle, it may be used to include the effects of superstructure nonlinearity (Sextos et al., 2003) by maintaining a linear model for the soil-foundation system. This simplifying assumption is acceptable if foundations are designed to avoid plasticization of piles.

### 2.1. Analysis of the Soil-Foundation System

The model proposed by Dezi et al. (2009) is used to perform the kinematic interaction analysis of the soil-foundation system and to obtain the dynamic impedance functions of the foundation. A generic group of piles with the same length embedded in a horizontally layered soil profile is considered; the analysis is performed in the frequency domain under the assumption of linear behaviour for both soil and piles. The problem is solved by modelling the piles with beam finite elements and the soil with independent horizontal infinite layers. The dynamic equilibrium condition of the pile group is thus expressed by the system of complex equations

$$\left[ \mathbf{K}_p - \omega^2 \mathbf{M}_p + \mathbf{Z}_p(\omega) \right] \mathbf{d}(\omega) = \mathbf{f}(\omega) \quad (2.1)$$

where  $\mathbf{K}_p$  and  $\mathbf{M}_p$  are the global stiffness and mass matrices of the piles, respectively.  $\mathbf{Z}_p$  is the global impedance matrix of the soil constructed by involving elastodynamic Green's functions defined on an infinite layer (Gazetas and Dobry, 1984; Dezi et al., 2009). Furthermore,  $\mathbf{d}$  is the vector grouping the nodal displacements and  $\mathbf{f}$  is the vector of the external loads due to the free-field motion. This approach allows capturing interactions between piles and the radiation damping in the unbounded soil. The presence of a rigid cap is simulated by introducing a rigid constraint with a master node having six degrees of freedom (three displacements and three rotations), collected in the vector  $\mathbf{d}_F$ . The final solving equation is

$$\begin{bmatrix} \mathbf{Z}_{FF} & \mathbf{Z}_{FE} \\ \mathbf{Z}_{EF} & \mathbf{Z}_{EE} \end{bmatrix} \begin{bmatrix} \mathbf{d}_F \\ \mathbf{d}_E \end{bmatrix} = \begin{bmatrix} \mathbf{f}_F \\ \mathbf{f}_E \end{bmatrix} \quad (2.2)$$

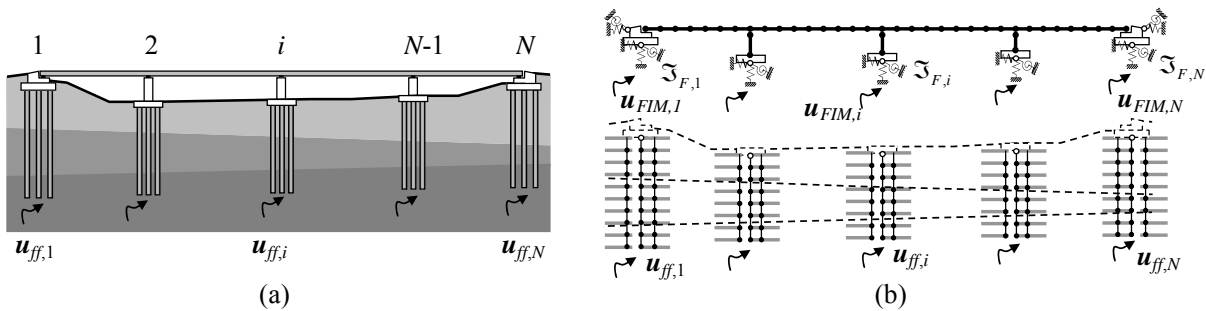


**Figure 2.1.** (a) Bridge founded on piles, (b) models of the superstructure on compliant-base and of the soil-foundation system

where the matrix  $\mathbf{Z}$  is obtained by manipulating and partitioning stiffness and mass matrices of Eqn. 2.1 accounting for the rigid constraint. The complex-valued foundation impedance matrix and the FIM are obtained condensating the problem

$$\mathfrak{Z}(\omega) = (\mathbf{Z}_{FF} - \mathbf{Z}_{FE} \mathbf{Z}_{EE}^{-1} \mathbf{Z}_{EF}) \quad (2.3)$$

$$\mathbf{d}_F(\omega) = \mathfrak{Z}^{-1} [\mathbf{f}_F - \mathbf{Z}_{FE} \mathbf{Z}_{EE}^{-1} \mathbf{f}_E] \quad (2.4)$$

These, according to the substructure approach, are necessary to perform the inertial interaction analysis of the superstructure. Pile displacements and stress resultants, due to seismic wave propagation in the soil, may also be computed at this stage. The procedure is straightforward once the free-field displacements within the deposit are known. Starting from a selected input motion, defined in a given location on the soil deposit, a propagation analysis is necessary to obtain the free-field displacements. Soil non-linearity may be considered both in the evaluation of the site response and in the subsequent kinematic interaction analysis, by adjusting soil stiffness and damping according to experimental curves taking into account the maximum strains attained.

## 2.2. Analysis of the superstructure

The inertial interaction analysis is carried out considering the structure on frequency dependent deformable restraints to capture both the compliance and the radiation damping of the soil-foundation system (Fig. 2.1b). However, in order to study nonlinear structures, analyses have to be performed in the time domain by substituting the soil-foundation system with LPMs constituted by frequency independent masses, springs and dashpots suitably assembled and calibrated (Wolf, 1988). Different procedures have been developed for the definition of complex LPMs capable of approximating impedances even characterized by multiple resonances (Wu and Lee, 2002). Nevertheless, in many practical cases simple LPMs are able to provide a good approximation; a model capable to capture the behaviour of pile groups characterized by roto-traslational coupling, that can be profitably used in bridge analysis, is shown in Fig. 2.2.

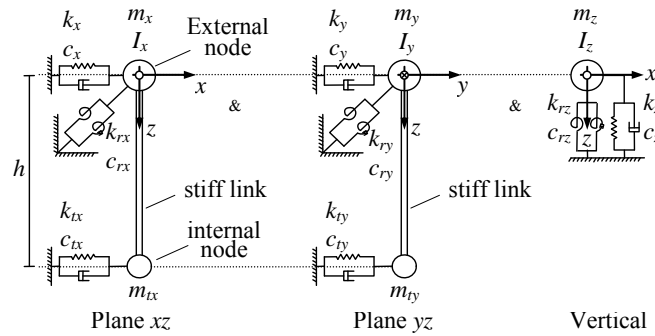


**Figure 2.2.** LPM with roto-traslational coupling

This LPM has 6 degrees of freedom and can be used for spatial analyses. The non-null components of the impedance matrix  $\tilde{\mathfrak{Z}}$  are ( $\alpha = x, y$ )

$$\tilde{\mathfrak{Z}}_{\alpha}(\omega) = [k_{\alpha} + k_{r\alpha} - \omega^2(m_{\alpha} + m_{r\alpha})] + i\omega(c_{\alpha} + c_{r\alpha}) \quad (2.5a)$$

$$\tilde{\mathfrak{Z}}_{r\alpha}(\omega) = [k_{r\alpha} + k_{\alpha}h^2 - \omega^2I_{\alpha}] + i\omega(c_{r\alpha} + c_{\alpha}h^2) \quad (2.5b)$$

$$\tilde{\mathfrak{Z}}_z(\omega) = [k_z - \omega^2m_z] + i\omega c_z \quad (2.5c)$$

$$\tilde{\mathfrak{Z}}_{rz}(\omega) = [k_{rz} - \omega^2I_z] + i\omega c_{rz} \quad (2.5d)$$

$$\tilde{\mathfrak{Z}}_{x-ty}(\omega) = h(k_{tx} - \omega^2m_{tx} + i\omega c_{tx}) \quad (2.5e)$$

$$\tilde{\mathfrak{Z}}_{y-rx}(\omega) = h(k_{ty} - \omega^2m_{ty} + i\omega c_{ty}) \quad (2.5f)$$

The 25 frequency-independent parameters are calibrated with a least squares procedure in order to achieve the better approximation of the foundation impedance functions in the frequency range in which the earthquake has the highest energy content and within which the fundamental structural vibration frequencies fall. Finally, seismic actions are applied at the base of the superstructure by considering time histories of forces acting at the master nodes of the pile groups computed by means of the inverse Fourier transform

$$\mathbf{f}_F(t) = \frac{1}{2\pi} \int_{-\infty}^{\infty} \tilde{\mathbf{z}}_F \mathbf{d}_F e^{i\omega t} d\omega \quad (2.6)$$

### 2.3. Remarks on the practical procedure

The procedure adopted makes it possible to perform analyses of bridges founded on piles, evaluating the effects of SSI both on the superstructure and on the foundations. It may be summarized in the following practical steps.

1. The free-field displacements at different depths, corresponding to the nodes of the finite element model of piles, are determined by means of a site response analysis for each soil profile, starting from a selected input motion. These analyses may be performed with the desired degree of detailing. In particular, 2D or 3D site response analyses may be considered to catch particular site configuration effects, otherwise, for practical purposes, 1D analyses may be carried out.
2. The FIM and the complex impedance matrix of each soil-foundation system are evaluated by means of the numerical model proposed by Dezi et al. (2009). The free-field motions within the soil profile, obtained from the previous step, constitute the seismic input for the analysis.
3. Suitable LPMs are defined to approximate the frequency dependent behaviour of the soil-foundation systems in order to perform the inertial interaction analysis of the superstructure in the time domain.
4. The superstructure is modelled and analyzed by exploiting potentials of dedicated computer software with the desired degree of sophistication (e.g. fiber elements, nonlinear hinges, geometrical nonlinearities). All the desired response quantities for the superstructure and the displacements of the foundation rigid caps are determined.
5. The stress resultants in the piles due to the kinematic and inertial interactions are computed.

## 3. APPLICATIONS

The previous procedure is adopted to investigate the effects of SSI in the seismic response of some viaducts. Analyses are carried out with reference to three bridges with different structural behaviour. In particular, 10-span viaducts with continuous steel-concrete composite decks are considered (Fig. 3.1a). The viaducts have a total length of 720 m with generic spans of 75 m and side spans of 60 m. The deck is constituted by a 12 m wide concrete slab, with mean thickness of 0.30 m, sustained by two 6 m spaced steel I-shaped beams having height equal to 2900 mm (Fig. 3.1b). The deck is supported on fixed bearings at the middle pier and on bearings fixed only in the transverse direction at the other piers; lock-up devices are adopted in the longitudinal direction to allow free elongations at service conditions. At the abutments multidirectional bearings are used in order to avoid a double-path resisting mechanism that would strongly involve the deck. Foundations are constituted by groups of bored concrete piles with 1200 mm diameter (Fig. 3.1c).

### 3.1. Seismic design of piers

In consideration of the deck restraint system, the seismic design is performed by considering a single pier that is studied as a SDOF system. The pier is clamped at the base and a direct displacement-based approach is used in order to control the ductility demand at Ultimate Limit State (ULS). The soil type D elastic displacement response spectrum defined by the Italian code NTC2008 is adopted by considering a Peak Ground Acceleration (PGA) of 0.47g (corresponding to 0.35g in soil type A). Pier of diameter 2.4 m and heights of 25, 15 and 10 m are sought to obtain different behaviours: pier with

height 25 m (H25) is expected to behave elastically while ductility demands  $\mu \approx 2$  and  $\mu \approx 4$  are expected for piers with heights 15 (H15) and 10 m (H10), respectively. Pier shear failures are prevented thanks to a suitable capacity design; concrete C35/45 and steel grade B450C are adopted. Reinforcement ratios (Fig. 3.1d) and detailing of structural elements comply with provisions of NTC2008.

A 40 m thick single layer soil deposit (Fig. 3.2a) constituted by normally consolidated clays with properties reported in Fig. 3.2c is considered. The variability with depth of the shear modulus at low strains ( $G_0$ ), from which the shear wave velocity profile is derived (Fig. 3.2b), is obtained according to empirical formulas available in the literature (Calabresi and Manfredini, 1976; D'Onofrio and Silvestri, 2001); the values of  $V_{s,30}$  (149 m/s) falls within the range defined by NTC2008 for soil type D. The deformable layer overlays a horizontal bedrock characterized by shear wave velocity  $V_{s,b} = 800$  m/s and density  $\rho_b = 2.2$  Mg/m<sup>3</sup>.

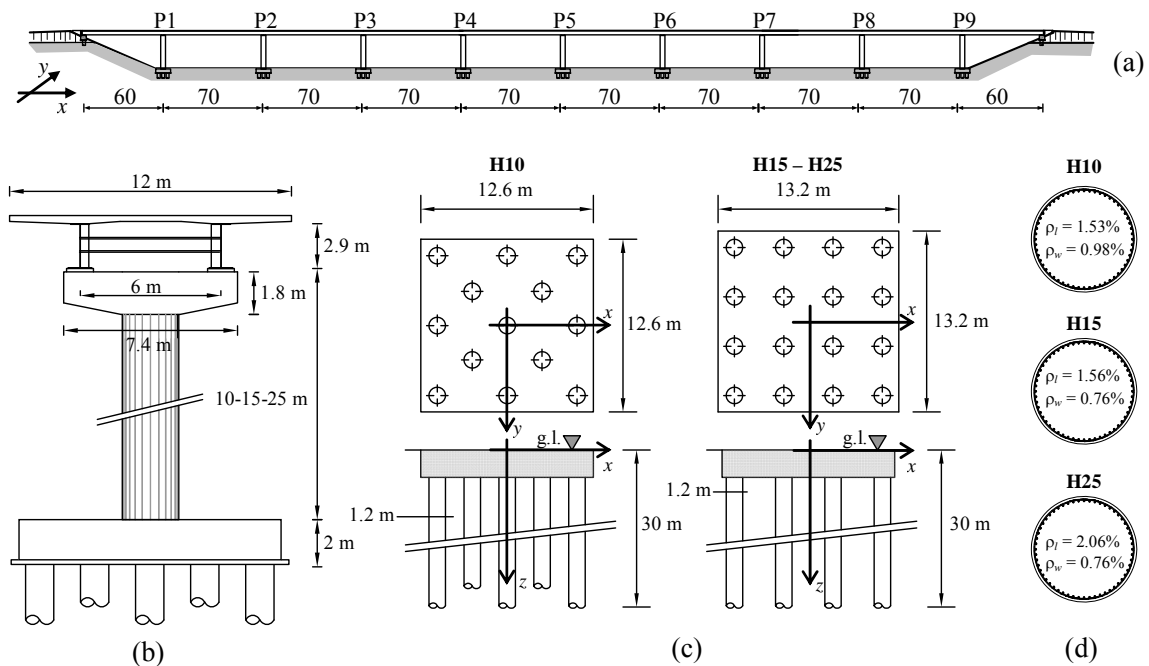


**Figure 3.1.** (a) Lateral view of the viaducts; (b) pier elevation; (c) foundations and (d) longitudinal and transverse reinforcement ratios of piers cross sections

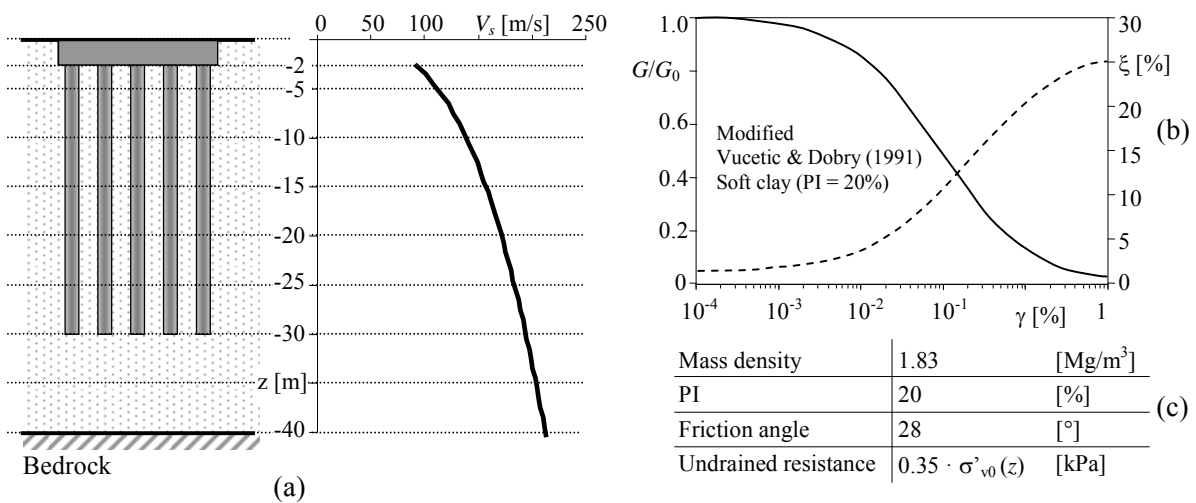


**Figure 3.2.** (a) Soil profile and  $V_s$  profile; (b) normalized shear modulus and damping ratio curves (c) soil mechanical properties

Foundations of piers are designed according to hierarchy principles in order to avoid the pile plasticization. As a consequence of the high seismicity level and the poor soil properties, a considerable number of piles is necessary to withstand the lateral actions that produce significant eccentricities of loads. For this purpose, about 30% of the bearing capacity of the foundation is entrusted to the rigid cap.

### 3.2. Kinematic interaction analysis and evaluation of foundation impedances

The analysis of the soil-foundation system is performed by means of the numerical model proposed by Dezi et al (2009) which allows obtaining the FIM and the frequency-dependent foundation impedances necessary for the subsequent inertial interaction analysis. Piles are modelled by 1 m long finite elements and are supposed to have density  $\rho_p = 2.5 \text{ Mg/m}^3$  and Young's modulus  $E_p \approx 23500 \text{ N/mm}^2$  to take into account concrete cracking. The seismic action is constituted by a set of six real records defined at the outcropping bedrock and selected so that their mean acceleration elastic response spectrum, normalised with respect to the PGA, matches the relevant spectrum suggested by the Italian NTC2008 for soil type A. Records, reported in Table 1, are then scaled in order to obtain a mean PGA of 0.35g, consistently with the hazard level considered in the design of viaducts. Each record includes two orthogonal horizontal components of the motion that are associated to the bridge longitudinal ( $x$ ) and transverse ( $y$ ) directions. Fig. 3.3 shows the mean displacement elastic response spectra of accelerograms (black continuous lines) compared with the reference spectrum of the code (black dotted line): in the transverse direction the code displacement spectrum is well reproduced up to a period of about 2 s after which the mean response spectrum of the selected accelerograms is about 120% higher; in the longitudinal direction, starting from a period of about 1 s, the mean spectrum of the selected records is about 50% higher than the code spectrum.

The transient seismic free-field motion within the deposit is obtained by means of a 1D site response analysis calibrating the soil shear modulus and damping consistently with the maximum strain level attained during the shaking; the modified curves of Vucetic and Dobry (1991) (Fig. 3.2 b) are adopted and the propagation analyses are performed separately in the two fundamental directions of the bridge. Fig. 3.3 shows the mean displacement elastic response spectra resulting at the ground surface (grey continuous lines), compared with the spectrum for soil type D (grey dotted line). It can be observed that site amplifications are evident in the whole period range; the code spectrum is reproduced quite closely up to the corner period (2 s) after which significant discrepancies are evident.

**Table 3.1.** Selected records

| Earthquake                 | Station                 | Date<br>[dd/mm/yy] | Magnitude<br>[ $M_w$ ] | PGA (y)<br>[g] | PGA (x)<br>[g] |
|----------------------------|-------------------------|--------------------|------------------------|----------------|----------------|
| Umbria-Marche (aftershock) | Nocera-Umbra Biscontini | 05/04/98           | 4.8                    | 0.101          | 0.225          |
| Friuli (aftershock)        | San Rocco               | 11/09/76           | 5.5                    | 0.090          | 0.089          |
| Campano Lucano 2°          | Sturno                  | 23/11/80           | 6.2                    | 0.078          | 0.071          |
| Campano Lucano 1°          | Torre del Greco         | 23/11/80           | 6.9                    | 0.063          | 0.040          |
| Campano Lucano 1°          | Bagnoli-Irpino          | 23/11/80           | 6.9                    | 0.139          | 0.202          |
| Campano Lucano 1°          | Sturno                  | 23/11/80           | 6.9                    | 0.358          | 0.251          |

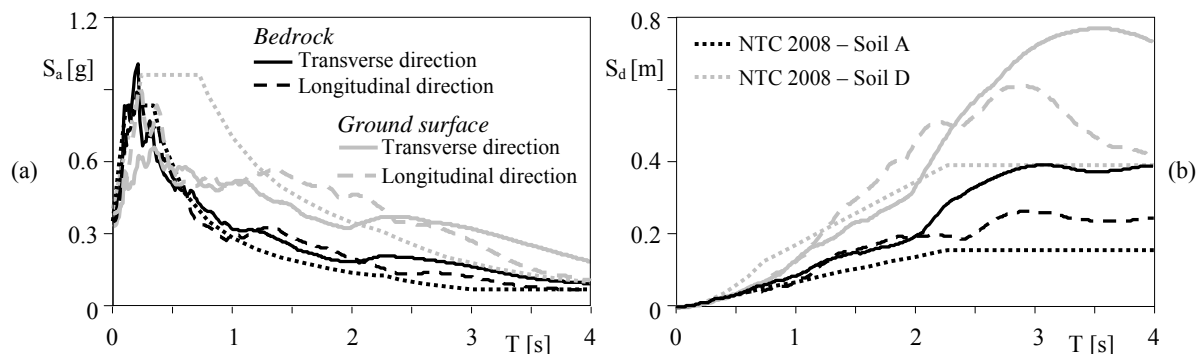


**Figure 3.3.** Mean response spectra of the selected accelerograms compared with reference spectra: (a) pseudo-accelerations and (b) displacements

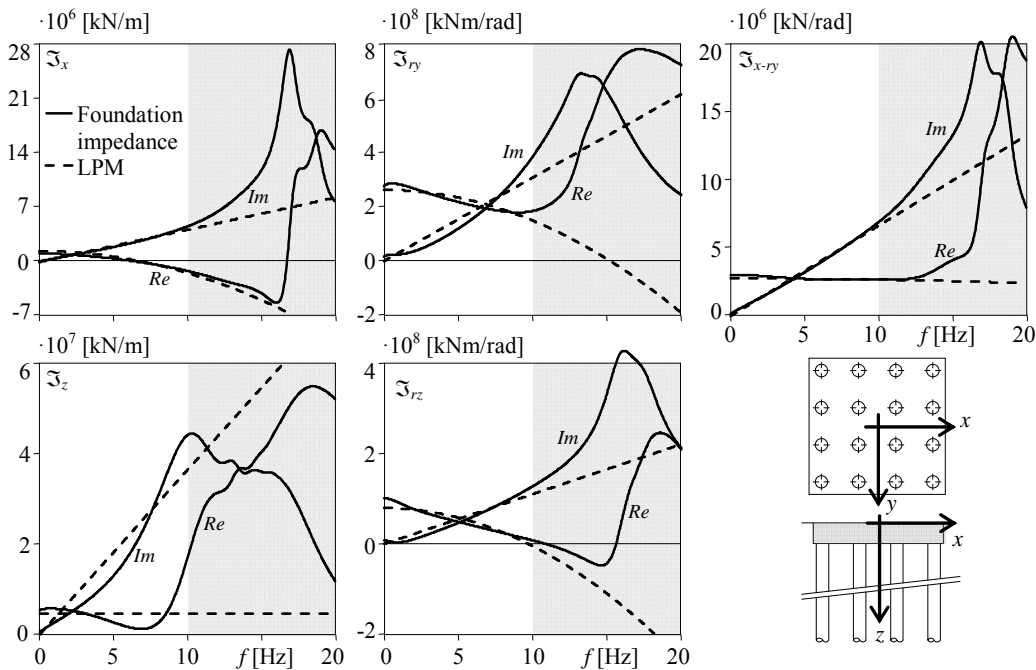


**Figure 3.4.** Non-null components of the impedance matrix of the soil-foundation system (viaducts H15 and H25)

The foundation of the single pier, subjected to the spatial free-field motion obtained by the site response analyses, is studied to evaluate the FIM. Interaction between piles of different foundations is neglected in view of the significant distance between piers. Furthermore, impedances of each pile group are evaluated; Fig. 3.4 shows the non-null components of the impedance matrix for the pier foundation of viaducts H15 and H25 (continuous lines).

### 3.3. Inertial interaction analysis of viaducts

Inertial interaction analyses are carried out considering the structures on frequency dependent compliant restraints. Three-dimensional finite element models are developed in Seismostruct (2007). Two different models are developed for each bridge: a Fixed Base (FB) model fully restrained at the base of piers, and a Compliant Base (CB) model obtained by introducing, at the base nodes, the LPMs previously defined. Beam elements with a linear elastic behaviour are used to model the steel-concrete composite deck accounting for the change of steel plate thicknesses along the deck and for the concrete cracking in the evaluation of the element mechanical properties. Piers are modelled with fiber elements in order to capture their nonlinear behaviour under bi-directional excitations; Mander's laws (1988) are considered for the confined and unconfined concrete while the constitutive model of Menegotto and Pinto (1973) is used for the reinforcement. Rigid links are suitably adopted to model the eccentricity between the pier and deck centroids. Furthermore, 5% structural damping is introduced in terms of tangent stiffness proportional damping. As for the soil-foundation system, the frequency dependent dynamic behaviour is taken into account by means of the LPM previously introduced. The constants are calibrated with a least squares procedure in order to achieve the better approximation of the impedance functions in the frequency range 0÷10 Hz; Fig. 3.4 shows (dashed lines) the non-null components of the LPM impedance matrix for the soil-foundation systems of viaducts H15 and H25.

## 4. RESULTS

In this section the effects of the SSI on the nonlinear seismic response of the bridges previously designed are discussed by comparing the results of the CB model with those obtained with the FB model. Unless otherwise specified, results refer to the mean values obtained from the nonlinear dynamic analyses performed with the set of real accelerograms.

### 4.1. Structural displacements and ductility demands

Structural displacements represent important performance parameters due to their strong correlation with damage. With reference to piers P1, P5 and P8, Figs. 4.1 and 4.2 show the displacements obtained from the FB and CB models of bridges H10 and H25, with 2 of the selected accelerograms. SSI increases displacements in both  $x$  and  $y$  directions as a consequence of the foundation compliance: effects are, as expected, more evident in bridge H10 characterised by stiffer piers, for which displacements increase up to 20% in the longitudinal direction. It is worth noting that displacements induced by the two accelerograms are quite different (about one order of magnitude). This is due to the set of earthquakes characterised by shakings with response spectra significantly scattered around the mean value.

Fig. 4.3 shows the maximum absolute displacements of the top of piers evaluated by averaging results of all the analyses considering the spatial components of the motion. Displacements thresholds corresponding to the first yielding of the pier reinforcements are reported with a dotted line. With reference to FB models, it can be observed that bridge H25 behaves almost elastically, according to the design assumptions, whereas bridges H15 and H10 undergo plastic deformations. Increments of displacements due to SSI increase, as already observed, by reducing the piers height; for bridge H10 displacements are, for the CB model, about 10% greater than those of the FB model.

Fig. 4.4 compares the displacement ductility demand of each pier with the relevant capacity; for the CB models, the effects of the foundation rigid rotation are suitably subtracted. It can be observed that, with reference to FB models, the ductility demand is close to the design one. SSI slightly increases the displacement ductility demand of piers as a consequence of the displacement increase; for the bridge H25, which is expected to remain in the elastic range, SSI slightly increases the plastic excursions; for bridge H10 the demand of edge piers becomes closer to the capacity.

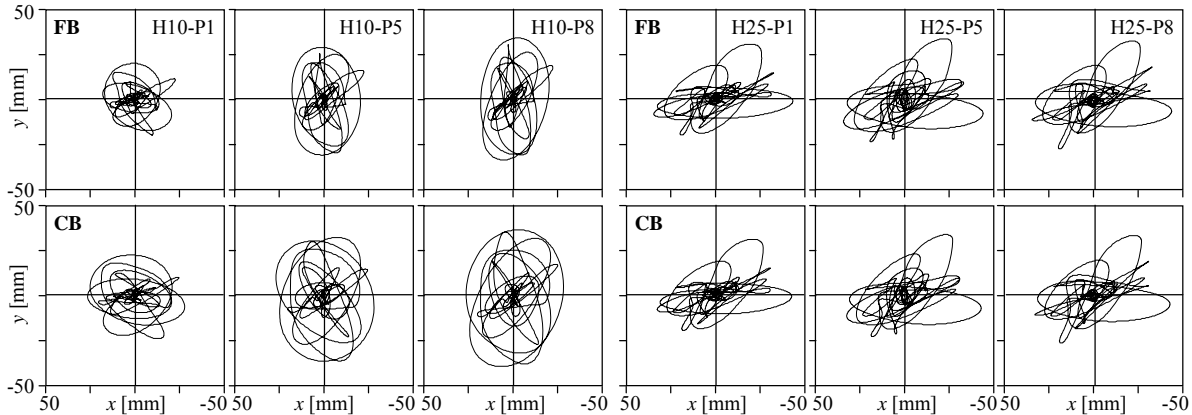


Figure 4.1. Displacements of piers P1, P5 and P8 for the Friuli earthquake (aftershock)

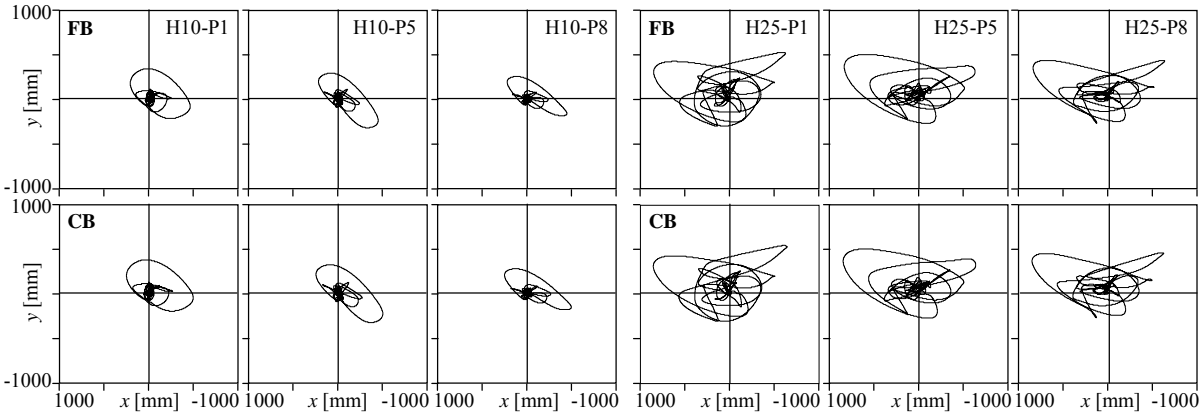


Figure 4.2. Displacements of piers P1, P5 and P8 for the Campano Lucano earthquake (Bagnoli-Irpino)

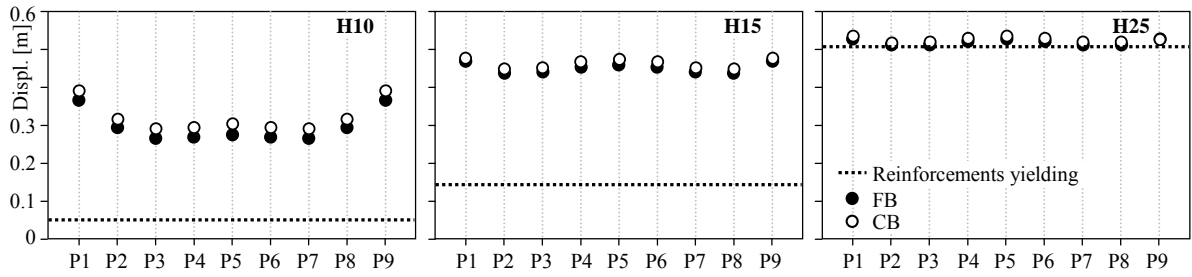


Figure 4.3. Maximum absolute displacements at the top of piers

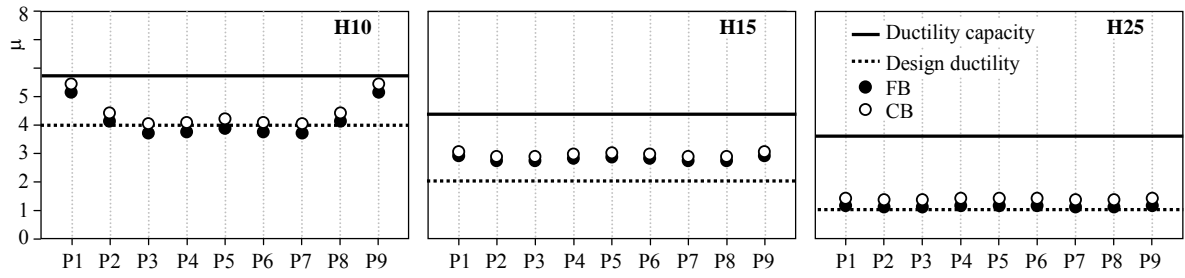


Figure 4.4. Ductility demands

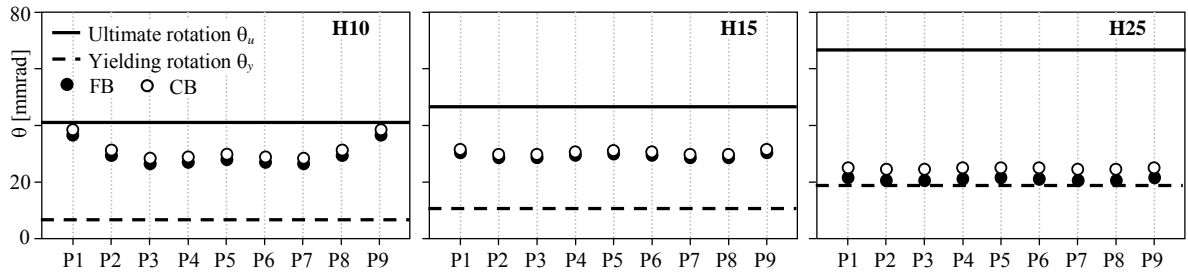


Figure 4.5. Rotation demands and capacity of plastic hinges

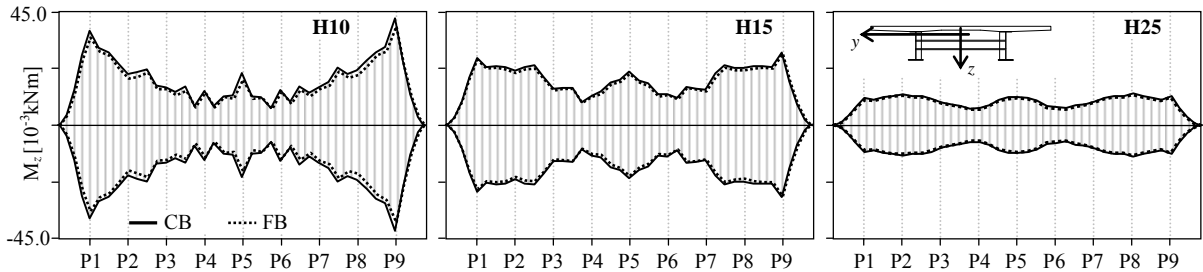


Figure 4.6. Deck transverse bending moments

#### 4.2. Piers plastic hinges rotation demands

Fig. 4.5 shows the rotation demands of plastic hinges at the base of the piers obtained by averaging results of the analyses performed on FB and CB models. In the graphs the yielding ( $\theta_y$ ) and the ultimate ( $\theta_u$ ) rotations calculated as suggested by Eurocode 8-2 by adopting the probable material properties are also reported; a safety factor  $\gamma_{R,p} = 1.4$  is considered for the ultimate plastic rotation. Even if the ultimate curvature increases by reducing the piers height (due to the axial force reduction and the greater amount of transverse reinforcement), the rotation capacity of plastic hinges decreases as a consequence of the reduction of plastic hinge length and yield rotation. As expected from the analysis of the transverse displacements, SSI increases the rotation demand of plastic hinges that, for the edge piers of bridge H10, are close to the rotation capacity. For bridge H25 increase of rotations due to SSI is probably more evident as a consequence of the early plastic behaviour of piers.

#### 4.3. Deck transverse bending moments

Fig. 4.6 shows the transverse bending moments of the deck obtained from the analyses of the FB and CB bridges. Such stress resultants increase by reducing the piers height as a consequence of the higher

stiffness of the substructures and of the differential displacements of the pier; the effects is particularly evident for the end spans, whereas the stress level for the middle spans is of the same order of magnitude for the three bridges. SSI always produces a very slight decrease of the transverse bending moments of the deck (the reduction appears more evident for bridge H10); however, as expected in consideration of the restraint layout that foresees multidirectional bearings at the abutments, the magnitude of the stress resultants are much lower than the deck yielding moment.

#### 4. CONCLUSIONS

In this paper some results of an ongoing research granted by the Italian Government is reported. It focuses on the effects of soil-structure interaction and proposes a comprehensive procedure for the analysis of bridges on pile foundations which integrates kinematic SSI of soil-foundation system and nonlinear inertial analysis of the superstructure. The first applications, aimed at the better understanding of the phenomena, are carried out on bridges founded on very soft soils in which including SSI is usually crucial in the evaluation of the seismic response. First results, obtained from a set of 3 bridges, demonstrate that SSI may increase the deck displacements up to 20% . On the other hand the ductility demand are only slightly increased by SSI without consequences on the capacity of substructures. The major design implications seem to be related to the expansion joints since the ductility demand of piers is only slightly affected by SSI. The upcoming developments of the research involve analyses on bridges characterised by different span lengths and including the effects of spatial variability of shakings.

#### ACKNOWLEDGMENTS

Support for this research from the Italian Government, PRIN 2008 fund, is gratefully acknowledged.

#### REFERENCES

- Calabresi G. and Manfredini, G. (1976). Terreni poco consistenti in Italia. *Rivista Italiana di Geotecnica*. **10:1**, 49-64.
- D'Onofrio A. and Silvestri F. (2001). Influence of micro-structure on small-strain stiffness and damping of fine grained soils and effects on local site response. *IV International Conference on 'Recent Advances in Geotechnical Earthquake Engineering and Soil Dynamics'*. S. Diego, CA. Paper 1.19.
- Dezi F., Carbonari S. and Leoni G. (2009). A model for the 3D kinematic interaction analysis of pile groups in layered soils. *Earthquake Engng Struct. Dyn.* **38: 11**, 1281-305.
- Gazetas G, Dobry R. (1984). Horizontal response of piles in layered soils. *Journal of Geotechnical Engineering ASCE*. **110**, 20-40.
- Mander J.B., Priestley M.J.N. and Park R. (1988). Theoretical Stress-Strain Model for Confined Concrete. *Journal of Structural Engineering ASCE*. **114:8**, 1804-826.
- Menegotto M., and Pinto P.E. (1973). Method of analysis for cyclically loaded R.C. plane frames including changes in geometry and non-elastic behaviour of elements under combined normal force and bending. *Symposium on the Resistance and Ultimate Deformability of Structures Acted on by Well Defined Repeated Loads*, Zurich, Switzerland, 15-22.
- NTC2008. (2008). Technical rules for constructions. (in Italian).
- Nuti C., Vanzi I. (2005). Influence of earthquake spatial variability on differential soil displacements and SDF system response. *Earthquake Engineering & Structural Dynamics* **34**, 1353-1374.
- SeismoSoft, SeismoStruct. (2007). A computer program for static and dynamic nonlinear analysis of framed structures, available from URL: <http://www.seismosoft.com>.
- Sextos A.G., Pitilakis K.D. and Kappos A.J. (2003). Inelastic dynamic analysis of RC bridges accounting for spatial variability of ground motion, site effects and soil-structure interaction phenomena. Part 2: Parametric study. *Earthquake Engng Struct. Dyn.* **32: 4**, 629-52.
- Vucetic M. and Dobry R. (1991). Effect of soil plasticity on cyclic response. *Journ. of Geot. Eng. ASCE*. **117:1**, 89-107.
- Wolf J.P. (1988). Soil-structure interaction analysis in time domain, Prentice-Hall, Englewood Cliffs, N.J.
- Wu W.H. and Lee W.H. (2002). Systematic lumped parameter models for foundations based on polynomial-fraction approximation. *Earthquake Engng Struct. Dyn.* **31: 7**, 1383-412.